Phenomenological models of the transient processes of diesel spray tip penetration

Xinyi Zhou[1, 2], Tie Li*[1, 2], Ping Yi[1, 2], Ning Wang[1, 2]
[1]State Key Laboratory of Ocean Engineering, Shanghai Jiao Tong University, Shanghai, PR China
[2]Institute of Power Plants and Automation, Shanghai Jiao Tong University, Shanghai, PR China
*Corresponding author email : litie@sjtu.edu.cn

Abstract
The multiple-injection strategy that has been used widely in diesel engines usually features a short duration for each injection pulse, which makes the start-of-injection (SOI) and end-of-injection (EOI) transients increasingly important for sprays in an injection event. Owing to the needle movement, spray developments during the transient processes are quite different from the spray at the quasi-steady state. In this paper, considering the sac pressurization processes during the SOI transients and effects of "entrainment wave" after the EOI, a theoretical zero-dimensional (0-D) model for the entire development processes of spray tip penetration is deduced. Then, the model is validated against the experimental spray data using a constant volume chamber and high-speed shadowgraphy. The model and experimental results demonstrate that the spray tip penetration has a $t^{3/2}$ dependence at the initial stage of injection rather than the t dependence suggested by the Hiroyasu model. Later, the spray tip penetration has a $t^{3/4}$ dependence owing to the spray breakup, a $t^{1/2}$ dependence with the completion of sac pressurization, and a $(t-t_i)^{1/4}$ dependence after two injection durations from the SOI[1].

Keywords
Diesel spray; Start-of-injection; End-of-injection; Spray tip penetration; 0-D models

Introduction

Spray tip penetration (S_{tip}) is one of the most important spray characteristics for diesel engines. As a result, accurate and quick calculation of S_{tip} is important for optimization of the spray combustion system. Because of its simplicity and ability to clearly reflect the effects of various design parameters, the 0-D model has been widely used in model-based optimization of diesel spray combustion systems.

With the assumption that the diesel spray is approximated as a gas jet, Wakuri et al. [1] developed a model for S_{tip} based on the theory of momentum conservation. They found that S_{tip} is proportion to the square root of time $t^{0.5}$. The $t^{0.5}$ dependence was verified by many studies [2]. Hiroyasu et al. [3] demonstrated that S_{tip} is initially proportional to the time t and then proportional to $t^{0.5}$. They derived a correlation based on Levich's jet disintegration theory [4]. Recently, the model constants of Hiroyasu's model were modified by Arai [5] for higher fuel injection pressures. Naber and Siebers [6] modified the Wakuri model [1] by considering a turbulent two-phase jet. According to their theoretical derivation, the dependence of S_{tip} upon the time gradually transitions from t to $t^{0.5}$, which confirms the correctness of Hiroyasu's model [3].

[1] t denotes the time after start of the fuel injection, and t_i the injection duration.

In the derivation processes of the above models, an idealized rectangular fuel injection rate profile was assumed [1-6], and the increase of sac pressure during the start-of-injection (SOI) transients and the termination of fuel momentum supply after the end-of-injection (EOI) were not considered. Recently, the above models were found to give an unacceptable prediction of S_{tip} during the SOI transients and after the EOI [7, 8]. These limitations seem to be acceptable when using a single long-pulsed fuel injection [1-6], where the SOI transients account for a relatively small proportion of the entire injection processes and the spray usually impinges upon the wall before the EOI. For modern diesel engines employing multiple-injection strategies, the SOI transients play an important role in the entire injection processes and spray evolution after the EOI can not be ignored, especially for the low temperature combustion that features in the early fuel injection. Therefore, further studies about S_{tip} during the SOI transients and after the EOI are needed.

Kostas et al. [9] studied S_{tip} during the initial 0.5 ms after SOI, and they found that S_{tip} follows an empirical correlation $S_{tip}(t) = At^{1.5}$ during the SOI transients. They suggested using their correlation in conjunction with Hiroyasu's correlation to describe the whole S_{tip} behaviour. Following the $t^{1.5}$ dependence suggested by Kostas et al. [9], Taşkiran et al. [10] modified the empirical correlation for the initial S_{tip} by considering the effects of injection pressure and ambient density. They confirmed that S_{tip} has a $t^{1.5}$ dependence at the injection startup. Recently, the authors of this paper proposed a theoretical model for S_{tip} during the SOI transients [8]. They reported that S_{tip} is proportional to $t^{1.5}$ at the acceleration stage, $t^{0.75}$ or t^{1} at the transition stage, and $t^{0.5}$ at the quasi-steady stage. They found that the model prediction results are in great agreement with the experimental data.

There are also many studies on spray evolution after the EOI. For example, Musculus et al. [11] developed a 1-D model for S_{tip} during the EOI transients. They reported that S_{tip} gradually transitions to be proportional to $t^{0.25}$ after two injection durations. Liu et al. [12] developed a 0-D model for S_{tip} during the EOI transients. They confirmed that S_{tip} is proportional to $t^{0.25}$ when the time is much longer than the injection duration. The time dependence $t^{0.25}$ has also been observed for a small quantity diesel spray [13] and water-jet [14]. The authors of this paper modified the fuel injection speed in Liu's model to the fuel injection pressure and made the changed model continuous with the Hiroyasu model at the time of two injection durations, and proposed a model for spray tail penetration based on the discrete control volume method [7]. Recently, Zhou et al. [15] studied the spray evolution during the EOI transient and compared various models developed so far. They reported that only the present authors' model [7] exhibits a trend close to the experimental results.

As reviewed in the above paragraph, although S_{tip} during the SOI and EOI transients have been studied to some extent, so far no models are summarized to predict the entire development processes of S_{tip}. More unfortunately, there are almost no data that can be used to develop and validate such a model. This is because the existing studies about the SOI and EOI transients are independent of each other. One of the objectives of this paper is to summarize the present authors' previous work on the transient diesel spray [7, 8] and further develop a model for the entire development processes of S_{tip}. Another objective is to provide experimental data to verify the newly developed model.

Model formulation

Figure 1(a) shows the conceptual models for the entire development process of S_{tip} when t_p is smaller than t_b. As can be seen, there are four key time points in the entire development process of S_{tip}: the sac pressurization time (t_p), breakup time (t_b), injection duration (t_i) and two injection durations ($2t_i$). Five stages can be divided according to these four time points: the

acceleration stage, transition stage 1, quasi-steady stage, transition stage 2 and decelerating stage.

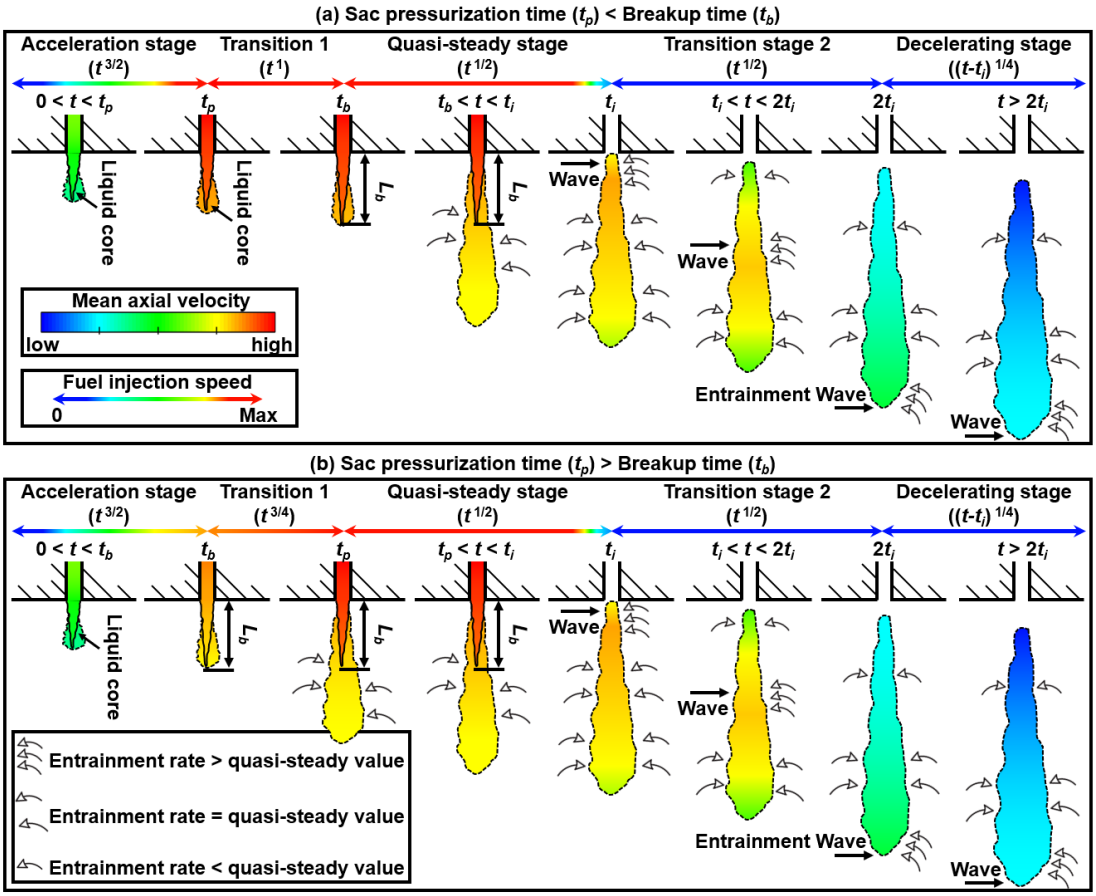

Figure 1. Conceptual models of the entire development processes of S_{tip}.

(1) At the acceleration stage ($0 < t \leq t_p$), the sac pressurization processes have not been completed and the liquid core is intact from the nozzle exit to the spray tip. During this time, the nozzle exit fuel velocity gradually increases and the increased fuel momentum at the nozzle exit would be easily transferred to the spray tip. As a result, S_{tip} exhibits an acceleration behavior during this stage.

(2) At the transition stage 1 ($t_p \leq t \leq t_b$), the sac pressurization processes has been completed but S_{tip} is still smaller than the breakup length. At this point, S_{tip} exhibits a linear dependence upon time, which is consistent with the Hiroyasu model before spray breakup.

(3) At the quasi-steady stage ($t_b \leq t \leq t_i$), since the breakup length is obviously shorter than the spray penetration length, S_{tip} during this stage is mainly controlled by fuel-air mixing. As a result, the late-injected fuel finds it is difficult to catch up to the early-injected fuel and S_{tip} exhibits a deceleration behavior.

(4) At the transition stage 2 ($t_i \leq t \leq 2t_i$), a disturbance of increased air entrainment termed the "entrainment wave" gradually travels downstream from the nozzle outlet to the spray tip. Since the "entrainment wave'' has not arrived, the spray tip still remains at the quasi-steady stage before $2t_i$ and the same model in the quasi-steady stage can be used.

(5) At the decelerating stage ($2t_i \leq t$), the whole spray enters into the decelerating state and the total momentum at the spray tip decreases with the time elapsing. As a result, the velocity of the spray tip is further reduced during this stage.

Figure 1(b) shows the conceptual models of the entire development processes of S_{tip} when t_p

is larger than t_b. S_{tip} behavior at the acceleration stage, quasi-steady stage, transition stage 2 and decelerating stage is consistent with the situation when t_p is smaller than t_b. At the transition stage 1 ($t_b \le t \le t_p$), the sac pressurization processes are still incomplete but S_{tip} is longer than the breakup length. The fuel moving inside the liquid core penetrates to the breakup length with negligibly small velocity loss, then the fuel moves to the spray tip with a gradually decreased velocity after breakup owing to the momentum exchange between the ambient air and fuel. As a result, although the nozzle exit fuel velocity still increases during this stage, S_{tip} exhibits a slight deceleration behavior.

As discussed in the above paragraphs, the Hiroyasu model [3] can be used at the quasi-steady stage and the transition stage 2. Based on the relationship among sac pressure, needle lift and time after start of injection (aSOI), the authors of this paper proposed a theoretical model for S_{tip} at the acceleration stage and the transition stage 1 [8]. Moreover, a theoretical model for S_{tip} at the decelerating stage is developed by the present authors [7]. Making the models in [3, 7-8] continuous at the turning points leads to

$$\begin{cases} 0 < t \le t_p & S_{tip}(t)=K_1(2\Delta P / t_p)^{1/2}\rho_f^{-1/2}t^{3/2} \\ t_p \le t \le t_b & S_{tip}(t)=K_1(2\Delta P / \rho_f)^{1/2}t \\ t_b \le t \le 2t_i & S_{tip}(t)=K_2(\Delta P / \rho_a)^{1/4}(d_n)^{1/2}(t)^{1/2} \\ 2t_i \le t & S_{tip}(t)=2^{1/2}K_2(\Delta P / \rho_a)^{1/4}(d_n)^{1/2}t_i^{1/4}(t-t_i)^{1/4} \\ t_b = K_{bt}(\rho_f d_n)(\rho_a \Delta P)^{-1/2} & K_2 = K_1(2K_{bt})^{1/2} \end{cases} \quad (1)$$

$$\begin{cases} 0 < t \le t_b & S_{tip}(t)=K_1(2\Delta P / t_p)^{1/2}\rho_f^{-1/2}t^{3/2} \\ t_b \le t \le t_p & S_{tip}(t)=K_2(\Delta P / t_p)^{1/4}\rho_a^{-1/4}(d_n)^{1/2}(t)^{3/4} \\ t_b \le t \le 2t_i & S_{tip}(t)=K_2(\Delta P / \rho_a)^{1/4}(d_n)^{1/2}(t)^{1/2} \\ 2t_i \le t & S_{tip}(t)=2^{1/2}K_2(\Delta P / \rho_a)^{1/4}(d_n)^{1/2}t_i^{1/4}(t-t_i)^{1/4} \\ t_b = K_{bt}(\rho_f d_n)(\rho_a \Delta P)^{-1/2} & \\ K_2 = 2^{1/2}K_1 K_{bt}^{3/4}\Delta P^{-1/8}t_p^{-1/4}\rho_f^{1/4}d_n^{1/4}\rho_a^{-1/8} & \end{cases} \quad (2)$$

here, t is the time after the start of injection [s]; ρ_a refers to the ambient density [kg/m^3]; d_n is the nozzle hole diameter [m]; $\triangle P$ indicates the difference between fuel injection pressure and ambient pressure [Pa]; ρ_f is the fuel density [kg/m^3]; K_1 and K_2 are the model constants; K_{bt} is the breakup time factor. Equation (1) is suitable when t_p is smaller than t_b, while Equation (2) is suitable when t_p is larger than t_b. It can be seen that both sides of Equations (1) and (2) can satisfy the conservation of dimensions, which verifies the correctness of the models.

According to Equations (1) and (2), S_{tip} shows a $t^{1.5}$ dependence upon time at the acceleration stage, t^1 or $t^{0.75}$ dependence at the transition stage 1, $t^{0.5}$ dependence at the quasi-steady stage and transition stage 2, and $(t\text{-}t_i)^{0.25}$ dependence at the decelerating stage. Since the exponent gradually decreases from 1.5 to 0.25, the spray tip experiences an acceleration process at the injection startup and then moves downstream at a gradually reduced speed.

Experimental setups

The Bosch long-tube method was used in the present study to measure the fuel injection rate, more details can be found in [16]. A constant volume combustion chamber (CVCC) was employed to measure the spray characteristics. The transient pressure in the CVCC was obtained by a pressure transducer (Kistler 6054B). One injector adapter was mounted on the head of the chamber, while five optical windows of 100 mm diameter can be mounted on the

bottom and sides of the chamber. Moreover, the distance from the nozzle outlet to the field of view was changed by using different injector adapters, as shown in **Figure 2**. In this study, the injector adapter 1 in **Figure 2(a)** was used to obtain S_{tip} between 0 to 90 mm (i.e. the spray upstream), while the injector adapter 2 in **Figure 2(b)** was used to obtain S_{tip} between 90 to 180 mm (i.e. the spray downstream). **Figure 2(c)** illustrates the diffused back-illumination (DBI) setup for imaging the temporal development of spray. An in-house light emission diode (LED) was adopted as the light source. After passing through a diffuser and the spray region, the light was captured by a CMOS camera coupled with a Nikon lens. One can refer to previous studies for more information about the optical arrangements [17]. Details about the imaging parameter settings and the experimental conditions are shown in **Table 1**.

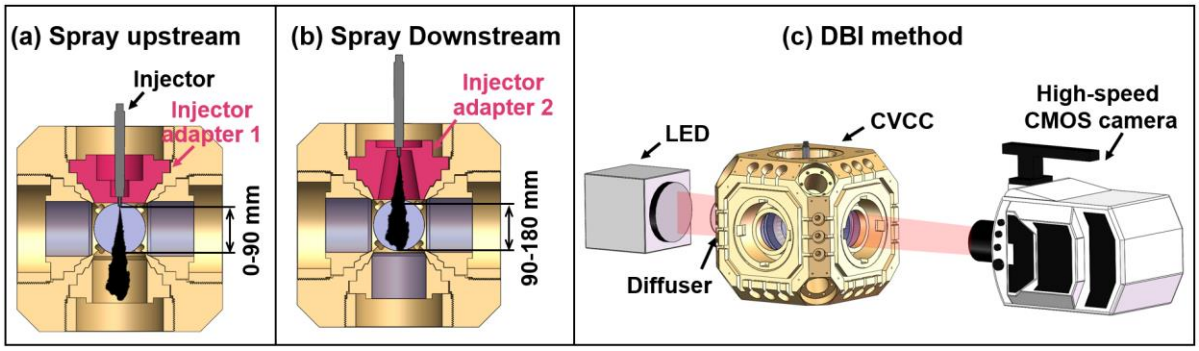

Figure 2. Experimental setups: (a) injector adapter 1 for the spray upstream; (b) injector adapter 2 for the spray downstream; (c) high-speed diffused back illumination imaging.

Table 1 - Experimental conditions and imaging settings.

Parameter	Value
Nozzle hole diameter (mm)	0.28
Fuel injection pressure (MPa)	120
Injection duration (ms)	2
Ambient density (kg/m^3)	20, 40, 60
Ambient temperature (K)	293
Ambient gas	Nitrogen
Imaging speed (fps)	80,000
Exposure time (μs)	1

Experimental results

Figure 3 shows the fuel injection rate profile with 120 MPa fuel injection pressure and 2 ms injection duration. According to the methods proposed in [8, 18], the sac pressurization time can be approximated as the time of the rapid increase of the injection rate at the injection startup. In this study, the sac pressurization time is determined to be 0.34 ms based on the ramp-up processes in **Figure 3**. **Figure 4(a)** shows the evolutions of S_{tip} under different ambient densities. The solid, half hollow and hollow symbols are used to distinguish the data from SOI to t_i, from t_i to $2t_i$, and after $2t_i$, respectively. Since the momentum exchange between the ambient air and fuel is enhanced at the higher ambient density, the S_{tip} decreases with the ambient density increasing. The spray tip velocity (V_{tip}) can be calculated by the derivative of S_{tip}, as given in **Figure 4(b)**. It can be seen that V_{tip} increases rapidly during the initial stage of injection and then gradually decreases to a lower value, which is consistent with the analyses of **Figure 1(b)**. During the acceleration stage, the liquid core is relatively intact, and V_{tip} mainly depends on the difference between fuel injection pressure and ambient pressure.

Since the ambient pressure is negligibly small compared to the fuel injection pressure, the effects of ambient density on V_{tip} is relatively small during the acceleration stage. After the acceleration stage, when S_{tip} is longer than the breakup length, the ambient air entrainment rate plays an important role in affecting V_{tip}. As a result, V_{tip} decreases with ambient density increasing after the acceleration stage. In the next section, the data in **Figure 4(a)** will be used to verify the newly developed model of this paper.

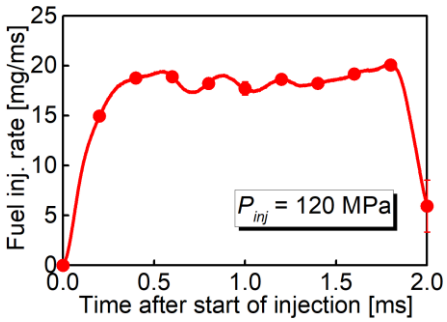

Figure 3. Fuel injection rate profile with 120 MPa fuel injection pressure and 2 ms injection duration

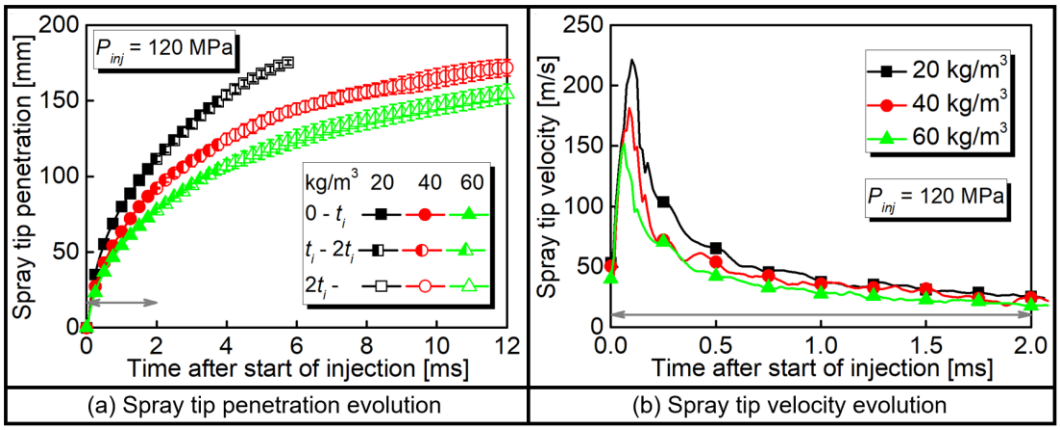

Figure 4. Spray tip penetration and spray tip velocity evolutions under different ambient densities.

Model evaluation

For the experimental conditions of this study, the sac pressurization time is larger than the breakup time. As a result, Equation (2) is applicable. Owing to the relationship between K_1 and K_2, there is only one model constant in Equation (2) that should be calibrated to consider the effects of different nozzle geometries. Calibrating K_1 against the experimental S_{tip} data, the optimal K_1 is 0.51 with the determination coefficient R^2 up to 98. 7%, as shown in **Figure 5**. It can be seen that the calculated results agree very well with the experimental data.

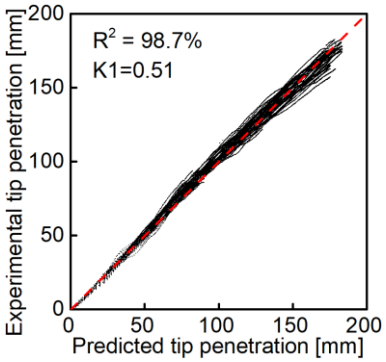

Figure 5. Comparison of S_{tip} between the experiment and calculation.

Figure 6 shows a comparison of the newly developed model and the Hiroyasu model under different ambient densities. The left side of **Figure 6** uses the linear coordinates to observe the overall evolution, while the right side uses logarithmic coordinates to better compare the predictability of these two models at the injection startup. The black, dark gray and light gray dots represent the experimental data from SOI to t_i, from t_i to $2t_i$ (i.e. the transition stage 2) and after $2t_i$ (i.e. the decelerating stage), respectively. Since the sac pressurization processes at the injection startup are not considered in the derivation processes, the Hiroyasu model overpredicts S_{tip} at the initial stage of injection. Moreover, the Hiroyasu model significantly overpredicts S_{tip} after $2t_i$, this is because that the quasi-steady fuel injection is assumed and the termination of fuel injection and fuel momentum supply is not considered in its derivation processes. Since the sac pressurization processes during the SOI transients and effects of "entrainment wave" after the EOI are considered, the newly developed model can predict the entire development processes of S_{tip}. It should be noted that K_{bt} of 28.65 suggested by Hiroyasu et al [3] is used for the newly developed model. As a result, in the logarithmic coordinates, the time of the first turning point of the newly developed model and the Hiroyasu model is consistent.

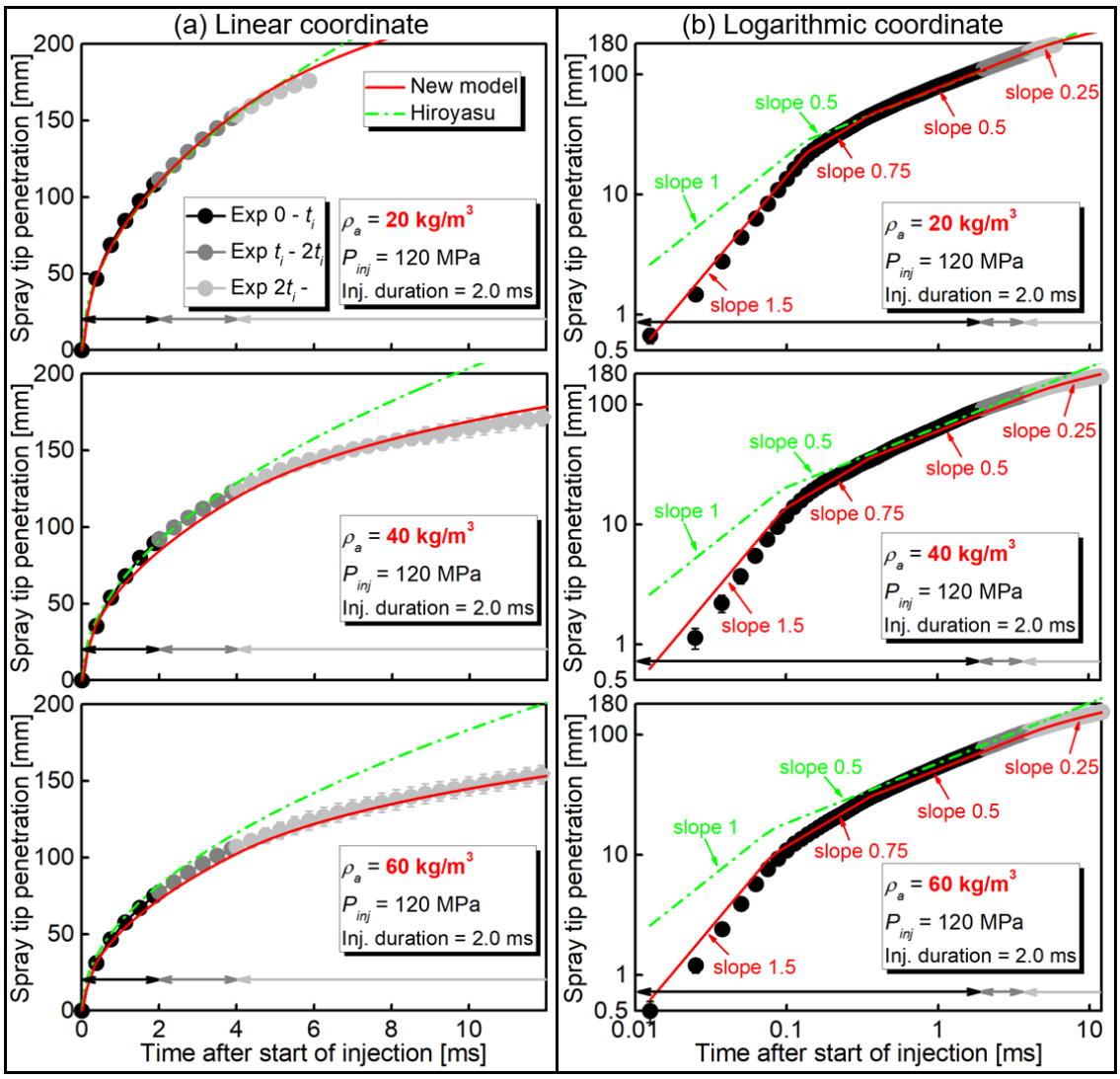

Figure 6. Model evaluation under the different ambient densities: (a) using the linear coordinate; (b) using the logarithmic coordinate.

Conclusions

The model and experimental results clarify four key time points in the entire development processes of S_{tip}: the sac pressurization time (t_p), breakup time (t_b), injection duration (t_i) and two injection durations ($2t_i$).

The entire development processes of S_{tip} can be summarized into five stages: the acceleration stage (S_{tip} proportion to $t^{1.5}$), transition stage 1 (t^1 or $t^{0.75}$), quasi-steady stage ($t^{0.5}$), transition stage 2 ($t^{0.5}$) and decelerating stage ($(t-t_i)^{0.25}$).

The calculated results of the newly developed model agree very well with the experimental data.

Acknowledgments

The supports by the Major International (Regional) Joint Research Project of National Natural Science Foundation of China (52020105009) are gratefully acknowledged.

Nomenclature

t	time after the start of injection [s]	t_p	sac pressurization time [s]
t_b	breakup time [s]	t_i	injection duration [s]
ρ_a	ambient density [kg/m^3]	d_n	nozzle hole diameter [m]
ρ_f	fuel density [kg/m^3]	K_{bt}	breakup time factor
K_1	model constant	K_2	model constant
SOI	start-of-injection	EOI	end-of-injection
$\triangle P$	difference between fuel injection pressure and ambient pressure [Pa]		

References

[1] Wakuri, Y., Fujii, M., Amitani, T., Tsuneya, R., 1960, Bull JSME, 3 (9), pp. 123-130.
[2] Desantes, JM., Payri, R., Salvador, FJ., Gil, A., 2006, Fuel, 85, pp. 910-917.
[3] Hiroyasu, H., and Arai, M., 1990, SAE paper 900475.
[4] Levich, VG., 1962, "Physicochemical Hydrodynamics."
[5] Arai, M., Aug. 23.-27. 2015, 13th International Conference on Liquid Atomization and Spray Systems.
[6] Naber, JD., and Siebers, DL., 1996, SAE paper 960034.
[7] Zhou, X., Li, T., Lai, Z., Wei, Y., 2019, Fuel, 237, pp. 442-456.
[8] Zhou, X., Li, T., Yi, P., 2020, International Journal of Engine Research, DOI: 10.1177/1468087420957852.
[9] Kostas, J., Honnery, D., Soria, J., 2009, Fuel, 88, pp. 2225-2237.
[10] Taşkiran, Ö. O., and Ergeneman, M., 2011, Journal of Combustion, 2011, 528126.
[11] Musculus, MPB., and Kattke, K., 2009, SAE paper 2009-01-1355.
[12] Liu, L., Ma, X., Magagnato, FA., 2017, Fuel, 199, pp. 324-331.
[13] Bao, Z., Horibe, N., Ishiyama, T., 2018, SAE paper 2018-01-0283.
[14] Sangras, R., Kwon, OC., Faeth, GM., 2002, Journal of Heat Transfer, 124 (3), pp.460-469.
[15] Zhou, Y., Qi, W., Zhang, Y., 2020, Energy, 211, 118605.
[16] Zhou, X., Li, T., Lai, Z., Wang, B., 2018, Fuel, 225, pp. 358-369.
[17] Zhou, X., Li, T., Wei, Y., Wang, N., 2020, International Journal of Engine Research, 21 (9), pp. 1662-1677.
[18] Zhou, X., Li, T., Yi, P., Zhang, Z., Wang, N., Wei, Y., 2020, Fuel, 276, 118026.